

Transmission of a human isolate of clade 2.3.4.4b A(H5N1) virus in ferrets

<https://doi.org/10.1038/s41586-024-08246-7>

Received: 10 July 2024

Accepted: 17 October 2024

Published online: 28 October 2024

 Check for updates

Joanna A. Pulit-Penalosa¹✉, Jessica A. Belser¹, Nicole Brock¹, Troy J. Kieran¹, Xiangjie Sun¹, Claudia Pappas¹, Hui Zeng¹, Paul Carney¹, Jessie Chang¹, Brandon Bradley-Ferrell¹, James Stevens¹, Juan A. De La Cruz¹, Yasuko Hatta¹, Han Di¹, C. Todd Davis¹, Terrence M. Tumpey¹ & Taronna R. Maines¹

Since 2020, there has been unprecedented global spread of highly pathogenic avian influenza A(H5N1) in wild bird populations with spillover into a variety of mammalian species and sporadically humans¹. In March 2024, clade 2.3.4.4b A(H5N1) virus was first detected in dairy cattle in the USA, with subsequent detection in numerous states², leading to more than a dozen confirmed human cases^{3,4}. In this study, we used the ferret, a well-characterized animal model that permits concurrent investigation of viral pathogenicity and transmissibility⁵, in the evaluation of A/Texas/37/2024 (TX/37) A(H5N1) virus isolated from a dairy farm worker in Texas⁶. Here we show that the virus has a remarkable ability for robust systemic infection in ferrets, leading to high levels of virus shedding and spread to naive contacts. Ferrets inoculated with TX/37 rapidly exhibited a severe and fatal infection, characterized by viraemia and extrapulmonary spread. The virus efficiently transmitted in a direct contact setting and was capable of indirect transmission through fomites. Airborne transmission was corroborated by the detection of infectious virus shed into the air by infected animals, albeit at lower levels compared to those of the highly transmissible human seasonal and swine-origin H1 subtype strains. Our results show that despite maintaining an avian-like receptor-binding specificity, TX/37 exhibits heightened virulence, transmissibility and airborne shedding relative to other clade 2.3.4.4b virus isolated before the 2024 cattle outbreaks⁷, underscoring the need for continued public health vigilance.

In recent years, clade 2.3.4.4b highly pathogenic avian influenza A(H5N1) viruses have exhibited rapid spread in wild bird populations, with sporadic but sustained detection in a diverse range of marine and terrestrial mammalian hosts across six continents^{8,9}. Several known human infections with 2.3.4.4b clade viruses have been documented since 2022 (ref. 4), resulting from confirmed or presumed exposure to infected animals or environments. Laboratory risk assessments of representative viruses have demonstrated the capacity for these viruses to cause severe mammalian infection, including an ability to transmit to serologically naive animals placed in close contact^{7,9–11}. For these reasons, public health risk assessments have been performed on clade 2.3.4.4b A(H5N1) viruses, and cross-reactive candidate vaccine viruses have been generated as a critical component of pandemic preparedness⁶.

In March 2024, clade 2.3.4.4b A(H5N1) virus infection was reported in dairy cattle in the USA, first in Texas with subsequent spread across several states by means of both interstate transport of infected animals and cow-to-cow transmission¹². Molecular clock analyses suggest that the virus emerged in cattle following a single avian-to-cattle introduction 3–5 months before its first detection². Infections with influenza A viruses (IAVs) have been exceptionally rare in bovine species, and hence bovines were not previously considered to be susceptible hosts for IAV^{13,14}. Since the first reports in cattle, multiple confirmed cases

have been reported in dairy farm workers with conjunctivitis or mild respiratory illness^{4,6}. Virus isolated in Texas (A/Texas/37/2024 (TX/37)) has high sequence identity to cattle isolates from geographically proximal areas, with the notable exception of PB2 E627K, a known molecular marker of host adaptation present in the human case from Texas but not in cattle isolates or other human cases to date⁶. Here we assessed the receptor-binding specificity of TX/37 and used the ferret model to evaluate the pathogenicity, transmissibility and airborne shedding of this virus.

TX/37 receptor-binding specificity

The switch in receptor specificity from sialic acid (SA) linked to galactose in α 2-3 linkages (avian) to α 2-6 linkages (human) has been shown to be a critical step for avian A(H5N1) IAV to adapt to mammals^{15–17}. Molecular analysis of the HA sequence of TX/37 showed that the residues of the receptor-binding site have high homology with other clade 2.3.4.4b avian and bovine isolates (Extended Data Fig. 1a). One amino acid difference outside the receptor-binding site was observed between TX/37 and New Mexico A(H5N1) virus (A/dairy cattle/New Mexico/A240920343-93/2024; cow/NM), which was reported to exhibit a preference for both avian- and human-like SAs¹⁸ (Extended Data Fig. 1b). Here, glycan microarray analysis consistently confirmed an avian α 2-3-linked SA specificity

¹Influenza Division, National Center for Immunization and Respiratory Diseases, Centers for Disease Control and Prevention, Atlanta, GA, USA. ✉e-mail: xzy5@cdc.gov

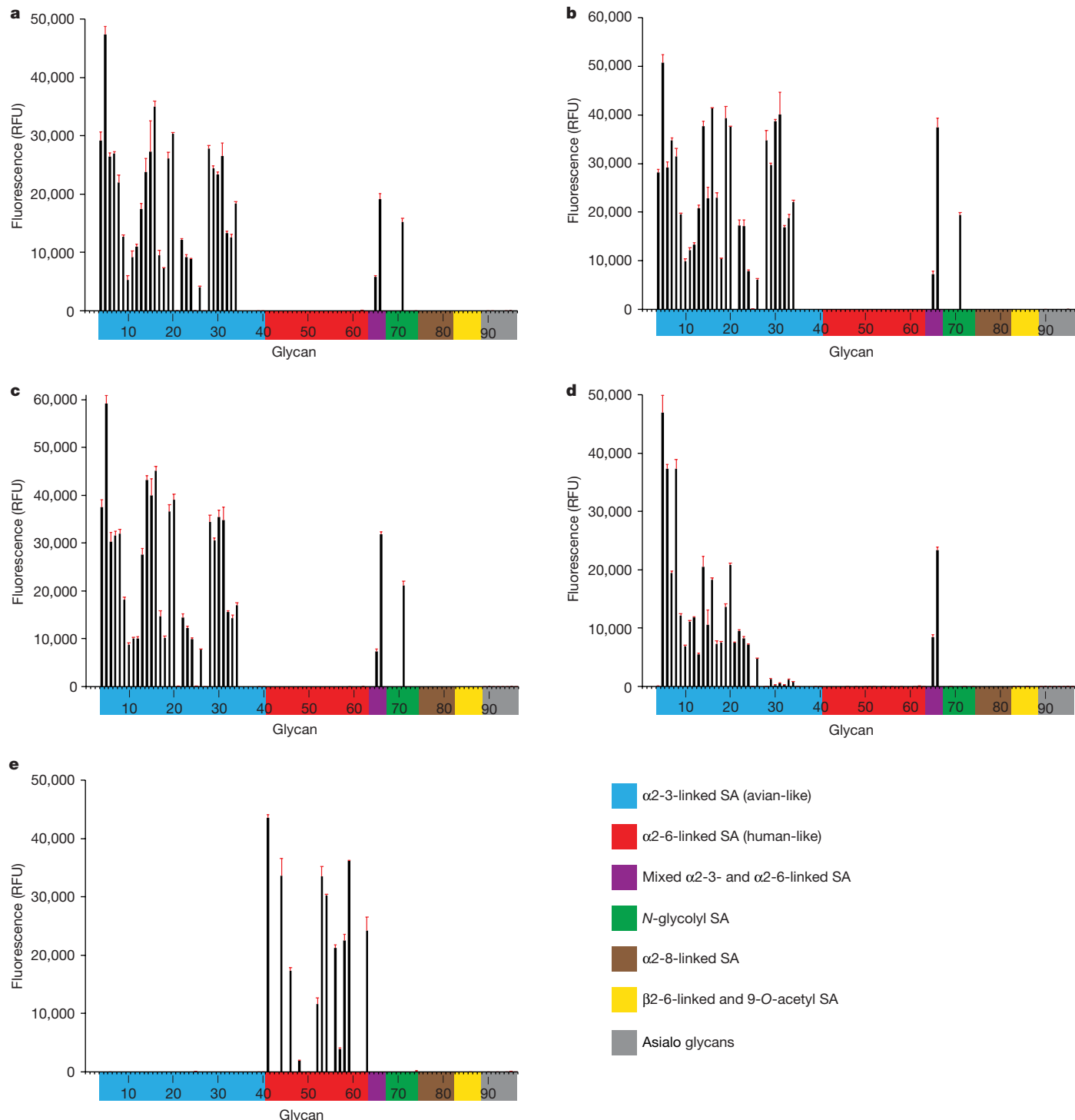


Fig. 1 | Glycan microarray analyses of recent clade 2.3.4.4b H5 recombinant HAs. **a–e**, Glycan microarray results for HA of clade 2.3.4.4b TX/37 A(H5N1) (**a**), clade 2.3.4.4b A/Sichuan/06681/2021 A(H5N1) (**b**), clade 2.3.4.4b A/Astrakhan/3212/2020 A(H5N1) (**c**), clade 1A/Vietnam/1203/2004 A(H5N1) (**d**) and seasonal

A/ Switzerland/9715293/2013 A(H3N2) (**e**). Coloured bars distinguish different glycan structures represented on the array. Error bars are standard deviations from six independent replicates on the array. RFU, relative fluorescent units. Each of the numbered glycans' structures is listed in Supplementary Table 1.

(Fig. 1a–d, glycans 4–40) for TX/37 and other representative H5 subtype viruses, in contrast to control human seasonal H3 subtype virus, which exhibited a strict human α2-6-linked SA binding preference (Fig. 1e, glycans 41–63). The only α2-6-linked SA-binding signals were from mixed α2-3- and α2-6-linked SA on the array (Supplementary Table 1, glycans 64–67). This lack of detectable binding to α2-6-linked SA was corroborated by an additional array that focused on the ability of HAs to bind to more representative human- and avian-type glycans, looking

at both length and avidity of binding with glycans spotted on the array at different concentrations (Supplementary Table 2). Binding to only α2-3-linked SA was detected, with shorter and biantennary glycans preferentially bound over longer and linear glycans (Extended Data Fig. 2a,b). Increased binding breadth could be attributed to amino acids near the receptor-binding site¹⁹. The HA of all of the recent clade 2.3.4.4b viruses showed a signal for an N-glycolylneuraminic acid-linked glycan, Neu5Gcα2-3Galβ1-4(Fucα1-3)GlcNAc (Fig. 1a–d, glycan 71).

Table 1 | Summary results of pathogenesis and transmission of TX/37 A(H5N1) virus in ferrets

Ferret group ^a	NW titre ^b	RS titre ^b	Weight loss (%) ^c	Temperature increase (°C) ^d	Lethargy ^e	Nasal discharge ^f	Ocular discharge ^f	Diarrhoea ^f	Mortality ^g	Seroconversion ^h
Inoculated	6.9 (12/12)	3.7 (10/12)	12.6 (12/12)	2.1 (12/12)	2.3	6/12	0/12	10/12	12/12 (2–3)	NT ⁱ
DC	3.9 (3/3)	1.6 (2/3)	6.1 (3/3)	1.6 (3/3)	1.9	0/6	0/3	3/3	3/3 (3–4)	NT ⁱ
FC	2.0 (1/3)	1.5 (1/3)	12.3 (1/3)	2.8 (1/3)	1.6	1/3	1/3	1/3	1/3 (9)	0/2 ^j
RDC	4.6 (4/6)	4.7 (4/6)	9.2 (4/6)	2.0 (4/6)	1.7	3/6	0/6	2/6	4/6 (4–6)	0/2 ^j

^aFerret groups—*inoculated*: ferrets intranasally inoculated with 6 log₁₀[PFUs] of TX/37. DC, direct contact ferrets; FC, fomite contact ferrets; RDC, respiratory droplet contact ferrets.
^bAverage maximum NW and RS titres expressed as log₁₀[PFUs ml⁻¹]; limit of detection 10 PFUs ml⁻¹. The number of ferrets with detectable virus over the total number of ferrets is in parentheses.
^cAverage weight loss on the day of euthanasia. Number of ferrets that exhibited weight loss over the total number of animals is in parentheses.
^dAverage maximum temperature increase over the baseline (36.7–38.8 °C).
^eRelative inactivity index.
^fNumber of ferrets with nasal discharge, ocular discharge or diarrhoea over the total number of animals.
^gNumber of animals euthanized during the experiment owing to severe signs of illness over the total number of animals. Day of euthanasia is shown in parentheses.
^hNumber of contact ferrets with antibodies to homologous virus in serum (seroconversion) over the total number of ferrets from which serum was collected.
ⁱAll ferrets with detectable TX/37 A(H5N1) virus in NWs did not survive the time course of infection; seroconversion was tested only in surviving animals; limit of detection <1:10; NT, not tested.

Although Neu5Gc-linked glycans are not believed to be receptors for IAVs, they are abundant in bovine tissues, including bovine mammary glands, which were shown to be the preferential site of replication of the A(H5N1) viruses in cows^{14,20}.

TX/37 pathogenicity in ferrets

Next we assessed the ability of TX/37 to infect and cause disease in the ferret model⁵. Following intranasal inoculation with a 6 log₁₀[plaque-forming unit (PFU)] dose of TX/37, ferrets rapidly developed severe disease, as evidenced by fever, weight loss, sustained diarrhoea, nasal discharge, laboured breathing and lethargy (Table 1 and Extended Data Fig. 3a–c). All inoculated animals succumbed to infection or necessitated humane euthanasia by day 2–3 post inoculation (p.i.), a more rapid decline than observed with previous 2.3.4.4b viruses isolated from animals and humans, which succumbed to infection between days 4 and 10 p.i. (refs. 7,9–11). TX/37 was detectable in ferret nasal wash (NW) and rectal swab (RS) samples at mean maximum titres of 6.9 and 3.7 log₁₀[PFUs ml⁻¹], respectively (Fig. 2a–c and Extended Data Fig. 4a–c). When subjected to post-mortem necropsy on day 3 p.i., all ferrets had high virus titres in systemic tissues, including the brain and gastrointestinal tract (Fig. 2d). Viraemia was observed in inoculated ferrets as early as 1-day p.i. (10–80 PFUs per millilitre of blood), contributing to the rapid systemic spread and accelerated fatal disease progression observed. The virus was also detected in the eye, conjunctiva and conjunctival washes collected from infected ferrets; however, overt inflammation of the conjunctiva was not noted (Fig. 2d and Extended Data Fig. 5).

TX/37 transmissibility in ferrets

Information on the transmissibility of newly emerging IAV in animal models is an important component of public health risk assessments^{21,22}. Here the capacity of TX/37 to transmit to naïve ferrets was evaluated using three experimental set-ups (direct contact, fomite contact and respiratory droplet contact ferret transmission models). Contact of the naïve ferret with the donor was established 24 h after inoculation of the donor ferrets, resulting in 30–48 h of total contact time. Efficient transmission was detected between all ferret pairs in the direct contact setting (3/3 contact ferrets). Virus was detected in NWs and RSSs collected from contact ferrets at mean maximum titres of 3.9 and 1.6 log₁₀[PFUs ml⁻¹], respectively (Table 1 and Fig. 2a). These contacts exhibited weight loss, fever, sustained diarrhoea, lethargy and laboured breathing, necessitating euthanasia by days 3–4 post contact (p.c.). The similarly rapid disease progression in both the inoculated donor and contact animals indicated that virus-inoculated animals were shedding high quantities of infectious virus into the

environment, leading to rapid exposure and infection of contact animals.

Recent work has shown that IAV can remain infectious in unpasteurized milk and on milking equipment materials for several hours^{23,24}, suggesting that exposure to contaminated surfaces may be contributing to the onward transmission of this virus. To test this, we used a fomite transmission model in which uninfected ferrets were placed in cages that had previously housed a virus-inoculated animal, so that the contact animal was exposed to cage walls, bedding, food and water that had been in direct contact with the inoculated ferret. The set-up was validated using four human seasonal and swine-origin H1 subtype viruses previously shown to be highly transmissible between ferrets placed in direct contact^{25,26}. Whereas the human seasonal virus exhibited efficient transmission following exposure to fomites, the three swine-origin viruses differed in their ability to transmit in this setting (Extended Data Fig. 6a–h). By contrast, a recently evaluated clade 2.3.4.4b A(H5N1) from Chile (A/Chile/25945/2023 (Chile/25945)) did not transmit in this setting⁷. When TX/37 was evaluated, transmission mediated by fomites occurred between one out of the three ferret pairs, as evidenced by the detection of virus in NW and RS samples and severe illness necessitating euthanasia of this animal on day 9 p.c. (Table 1 and Fig. 2b). The transmission outcome was accompanied by the detection of infectious virus in the air collected from the cage on the day of the first cage swap and in a cage swab sample collected on the day of the second cage swap (Extended Data Fig. 7a–c). However, the virus found on cage surfaces was largely non-infectious, suggesting that high levels of airborne infectious viral particles originating from the contaminated cage (for example, stirred up bedding and dander) could have contributed to the observed transmission.

We then assessed transmission mediated by respiratory droplets, a model in which all forms of direct and indirect contact are eliminated. In this setting, virus transmission was less efficient than in the presence of direct contact; four out of the six contact ferrets began exhibiting signs of infection on day 4 p.c., as evidenced by weight loss, fever and lethargy. Virus was detected in NW and RS samples from contact animals at mean maximum titres of 4.6 log₁₀[PFUs ml⁻¹] and 4.7 log₁₀[PFUs ml⁻¹], respectively. Although the exposure dose is typically lower in this more stringent setting, all contacts with detectable virus in NWs met humane endpoint criteria by day 4–6 p.c. (Table 1 and Fig. 2c). The remaining two contacts showed no signs of disease and remained seronegative to TX/37 at day 21 p.c., indicating that productive transmission did not occur.

Irrespective of the transmission mode assessed, all contact animals with detectable virus in NWs developed severe and fatal disease. Overall, viraemia and high-titre systemic detection of virus were observed in tissue samples from all contacts (Extended Data Fig. 8a,b). Similar to what was observed in samples from inoculated ferrets, no genetic

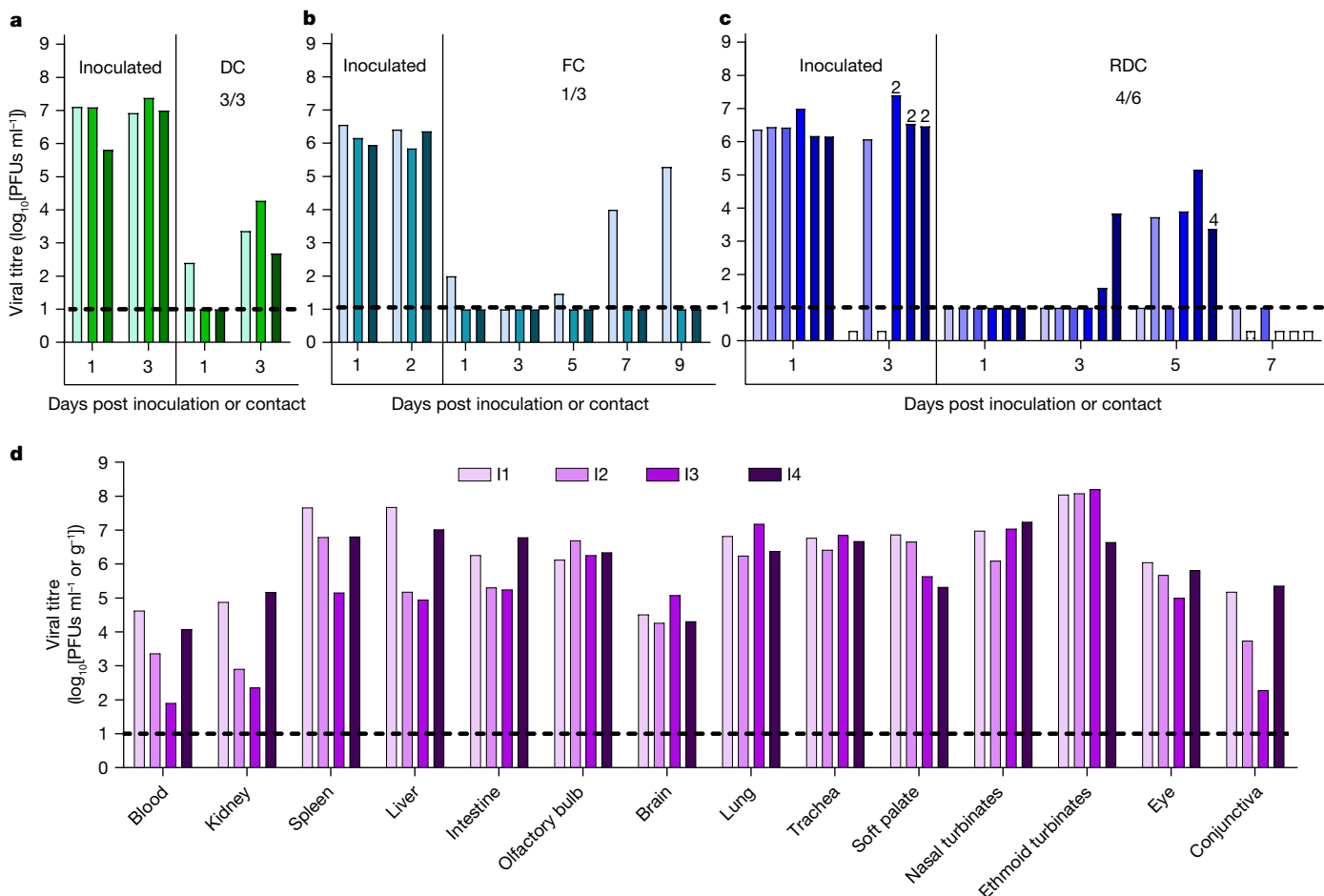


Fig. 2 | Transmission and pathogenesis of TX/37 A(H5N1) in the ferret model. Ferrets were inoculated with $6 \log_{10}[\text{PFUs}]$ of TX/37. Contact was established 24 h after inoculation of the donor ferrets, resulting in 30–48 h of total contact time (until euthanasia of the inoculated ferrets on day 2–3 p.i.). **a–c**, Transmission settings: direct contact (one inoculated and one naïve ferret co-housed in one cage; three pairs; **a**), indirect (fomite) contact (one inoculated and one naïve ferret housed in alternating cages; cage swaps performed once daily; three pairs; **b**) and respiratory droplet contact (one inoculated and one naïve ferret housed in adjacent cages; six pairs; **c**). Transmission to naïve contacts was evaluated by the detection of virus in NWs. Samples were collected every

other day post inoculation or contact, or on the day of euthanasia (day 2 or day 4 indicated on top of the bar). Bars with no colour denote animals that succumbed to infection before sample collection. **d**, Virus dissemination in tissues was evaluated in samples from four inoculated animals (I1–4) on day 3 p.i. Viral titres are reported at $\log_{10}[\text{PFUs ml}^{-1}]$ (blood, soft palate, nasal turbinates, ethmoid turbinates, eye, conjunctiva) or $\log_{10}[\text{PFUs g}^{-1}]$ (of tissue; kidney, spleen, liver, intestines, olfactory bulb, brain, lung, trachea). The limit of detection is 10 PFUs ml^{-1} or g^{-1} ; dashed line. Each bar represents an individual ferret.

changes at known mammalian adaptation markers were detected in samples collected from the contacts. Detected variants were not consistently enriched in contact animals, suggesting that transmission was not attributed to changes in TX/37 sequence (Supplementary Table 3). Collectively, these studies support the capacity for TX/37 to transmit to serologically naïve mammals by a variety of modes, including the airborne route, although the relative efficiency of transmission varied on the basis of the setting.

TX/37 airborne release in ferrets

In addition to its detection in cattle, clade 2.3.4.4b A(H5N1) virus has been reported in multiple other mammals and gallinaceous poultry on affected farms, including cats, raccoons and opossums^{2,12,27}, indicating interspecies transmission. Although our findings and others support the ability of some wild-type A(H5N1) strains to spread among ferrets in close contact, airborne transmission as seen here with TX/37, has not been observed^{7,9–11,28,29}. To more closely examine the relative ability of this virus to spread through the air, we collected airborne respiratory particles shed by TX/37-infected ferrets, to quantify infectious virus

and viral RNA present in the air, using both a cyclone-based sampler (BC 251) and a water condensation sampler (SPOT). The results were compared to a 2023 2.3.4.4b A(H5N1) virus, Chile/25945, that was isolated from a human and did not transmit by the airborne route⁷, as well as human seasonal A(H1N1) and swine-origin A(H1N2)v viruses, previously shown to be highly transmissible among ferrets^{25,30}. All of the tested viruses were capable of robust replication in the ferret model and were detected in NWs at comparable infectious virus titres (Supplementary Table 4), with high virus levels detected early (days 1–2 p.i.), in agreement with studies supporting the critical timing of virus transmission in this model^{31–34}. However, infectious virus levels in the air were significantly higher and detected to day 3 p.i. (up to 246 PFUs h^{-1}) for the H1 subtype viruses as compared to Chile/25945. This virus was detectable at low levels ($1–16 \text{ PFUs h}^{-1}$) only on day 1 p.i., further supporting its inability to transmit through the airborne route in ferrets⁷. TX/37 detection peaked later as compared to that of the well-adapted H1 viruses. The virus was detected in the air on both day 1 and 2 p.i. with most air samples containing higher titres of infectious virus ($1–52 \text{ PFUs h}^{-1}$ on day 1 p.i. and $9–109 \text{ PFUs h}^{-1}$ on day 2 p.i.) relative to the titres observed in the Chile/25945 samples (Fig. 3a–d).

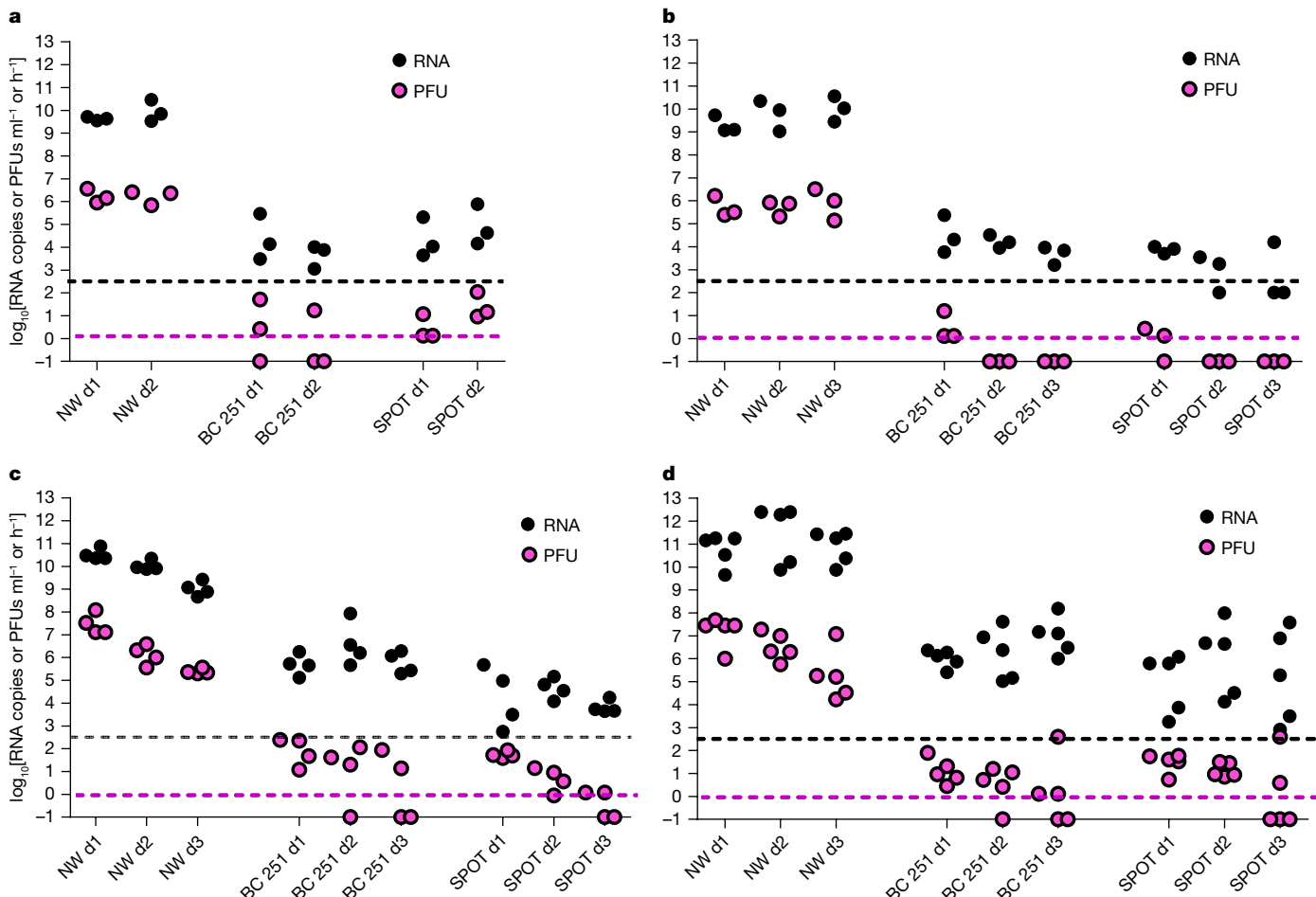


Fig. 3 | Detection of airborne influenza virus released from inoculated ferrets. **a–d.** Ferrets were inoculated intranasally with $6 \log_{10}[\text{PFUs}]$ of clade 2.3.4.4b TX/37 A(H5N1) (**a**), clade 2.3.4.4b Chile/25945 A(H5N1) (**b**), human seasonal A/Nebraska/14/2019 A(H1N1) (**c**) and swine-origin A/Minnesota/45/2016 A(H1N2)v (**d**). Virus titres in NW samples collected from individual inoculated ferrets are shown on the left side of each graph. Virus titres in NWs were evaluated using standard plaque assay to determine infectious virus load (pink circles; limit of detection 10 PFUs ml^{-1}) and real-time quantitative PCR with reverse transcription to determine viral RNA load (black circles; limit of detection $2.9 \log_{10}[\text{RNA copies ml}^{-1}]$). Aerosol samples were collected from each inoculated animal ($n = 3\text{--}5$ per virus) daily for 3 days p.i. (or until

euthanasia; day 2 (d2) for TX/37) for 1 h using a BC 251 sampler (3.5 l min^{-1}) and a SPOT sampler (1.5 l min^{-1}), sequentially. Infectious virus was analysed by plaque assay (limit of detection 1 PFU h^{-1} , dashed pink line with negative samples shown below the line; the BC 251 data represent infectious virus recovered in the $>4\text{-}\mu\text{m}$ sampler fraction, no infectious virus was recovered from the fractions containing aerosol particles of $1\text{--}4\text{ }\mu\text{m}$, or $<1\text{ }\mu\text{m}$) and viral RNA in each sample was quantified using real-time quantitative PCR with reverse transcription (limit of detection $2.5 \log_{10}[\text{RNA copies h}^{-1}]$, dashed black line with negative samples shown below the line; the BC 251 data represent the sum from all three sampler fractions). Statistical analysis is reported in Supplementary Table 4.

These results suggest that TX/37 is shed in the air at levels sufficient to support the airborne transmissible phenotype observed.

Discussion

To cause a pandemic, an influenza virus must be immunologically distinct from previous circulating strains, be able to productively infect humans, and be able to spread efficiently among humans³⁵. Like many other animal-origin IAVs associated with documented zoonotic human infection, clade 2.3.4.4b A(H5N1) viruses meet two of these criteria at present but lack the capacity to spread person-to-person. However, transmission of the virus in multiple mammalian species affords opportunities for the virus to adapt and become capable of meeting all three pandemic criteria³⁶. Although sustained human-to-human transmission of A(H5N1) has not been detected so far, epidemiologic reports suggest that interspecies transmission from infected dairy cattle to other mammals is taking place².

Here we show that TX/37 was capable of rapidly causing fatal, systemic infection in naive ferrets, as related clade 2.3.4.4b viruses did in

infected cats on dairy farms²⁷. However, extrapolation of our findings to the human population at large should proceed with caution as multiple factors may contribute to disease outcome. As humans lack widespread immunity to H5 subtype viruses, investigation of pre-existing IAV immunity (especially due to N1 neuraminidase) may shed light on the mild human cases reported in dairy workers in the USA so far³⁷. In addition, studies presented here were conducted with young male ferrets, and high inoculation doses were tested; viral pathogenicity can be age and sex dependent and modulated by comorbidities, exposure routes and doses^{38–40}, which all require further evaluation. Unlike other human and bovine isolates associated with outbreaks on dairy farms, TX/37 possesses a mammalian adaptation marker in PB2, E627K, which has been shown to enhance virulence and transmission in ferrets⁴¹. As recent reports suggest that bovine isolates with sequences highly homologous to TX/37 but lacking that substitution in PB2 may also have capacity for lethal infection and limited transmission in ferrets^{18,37}, further investigation of additional bovine and human isolates is needed to better understand the overall public risk associated with the A(H5N1) viruses that emerged in cattle. In addition, notable differences in the sequences

of bovine outbreak-related viruses and other clade 2.3.4.4b strains (for example, the presence of Q591K and D701N instead of E627K in PB2 of Chile/25945; (Supplementary Table 5) require further investigation to fully appreciate the role of strain-specific variability in airborne virus shedding and transmission phenotypes among A(H5N1) viruses circulating at present.

Our work reporting the shedding of diverse IAVs into the air using two distinct airborne particle collection approaches in the ferret model offers an advancement in our understanding of the role that infectious virus shed early after infection plays in onward transmission. The optimization and inclusion of aerobiological sampling in risk assessments can thus enhance our ability to identify strains with increased airborne transmission potential. Despite the severe disease and enhanced transmission exhibited by the TX/37 virus studied here in the ferret model, our results indicate that the virus maintains avian-like receptor-binding specificity and, therefore, would require further adaptation to augment its pandemic potential. Nonetheless, continued monitoring of the evolution of A(H5N1) viruses, especially those isolated from humans, and the animals to which humans are frequently exposed, is a critical component of pandemic preparedness.

Online content

Any methods, additional references, Nature Portfolio reporting summaries, source data, extended data, supplementary information, acknowledgements, peer review information; details of author contributions and competing interests; and statements of data and code availability are available at <https://doi.org/10.1038/s41586-024-08246-7>.

1. Gilbertson, B. & Subbarao, K. Mammalian infections with highly pathogenic avian influenza viruses renew concerns of pandemic potential. *J. Exp. Med.* **220**, e20230447 (2023).
2. Nguyen, T.-Q. et al. Emergence and interstate spread of highly pathogenic avian influenza A(H5N1) in dairy cattle. Preprint at *bioRxiv* <https://doi.org/10.1101/2024.05.01.591751> (2024).
3. Garg, S. et al. Outbreak of highly pathogenic avian influenza A(H5N1) viruses in U.S. dairy cattle and detection of two human cases - United States, 2024. *MMWR Morb. Mortal. Wkly Rep.* **73**, 501–505 (2024).
4. Avian Influenza (Bird Flu) (Centers for Disease Control and Prevention, accessed 7 November 2024); <https://www.cdc.gov/bird-flu/situation-summary/index.html>.
5. Belser, J. A., Eckert, A. M., Tumpey, T. M. & Maines, T. R. Complexities in ferret influenza virus pathogenesis and transmission models. *Microbiol. Mol. Biol. Rev.* **80**, 733–744 (2016).
6. Uyeki, T. M. et al. Highly pathogenic avian influenza A(H5N1) virus infection in a dairy farm worker. *N. Engl. J. Med.* <https://doi.org/10.1056/NEJMc2405371> (2024).
7. Pulit-Penalosa, J. A. et al. Highly pathogenic avian influenza A(H5N1) virus of clade 2.3.4.4b isolated from a human case in Chile causes fatal disease and transmits between co-housed ferrets. *Emerg. Microbes Infect.* **13**, 2332667 (2024).
8. Graziosi, G., Lupini, C., Catelli, E. & Carnaccini, S. Highly pathogenic avian influenza (HPAI) H5 clade 2.3.4.4b virus infection in birds and mammals. *Animals* **14**, 1372 (2024).
9. Kandeil, A. et al. Rapid evolution of A(H5N1) influenza viruses after intercontinental spread to North America. *Nat. Commun.* **14**, 3082 (2023).
10. Maemura, T. et al. Characterization of highly pathogenic clade 2.3.4.4b H5N1 mink influenza viruses. *eBioMedicine* **97**, 104827 (2023).
11. Restori, K. H. et al. Risk assessment of a highly pathogenic H5N1 influenza virus from mink. *Nat. Commun.* **15**, 4112 (2024).
12. Avian Influenza (Animal and Plant Health Inspection Service, United States Department of Agriculture, accessed 16 June 2024); <https://www.aphis.usda.gov/livestock-poultry-disease/avian/avian-influenza>.
13. Sreenivasan, C. C., Thomas, M., Kaushik, R. S., Wang, D. & Li, F. Influenza A in bovine species: a narrative literature review. *Viruses* **11**, 561 (2019).
14. Rios Carrasco, M., Grone, A., van den Brand, J. M. A. & de Vries, R. P. The mammary glands of cows abundantly display receptors for circulating avian H5 viruses. *J. Virol.* **98**, e01052-24 (2024).
15. Stevens, J. et al. Structure and receptor specificity of the hemagglutinin from an H5N1 influenza virus. *Science* **312**, 404–410 (2006).
16. Imai, M. et al. Experimental adaptation of an influenza H5 HA confers respiratory droplet transmission to a reassortant H5 HA/H1N1 virus in ferrets. *Nature* **486**, 420–428 (2012).
17. Herfst, S. et al. Airborne transmission of influenza A/H5N1 virus between ferrets. *Science* **336**, 1534–1541 (2012).
18. Eisfeld, A. J. et al. Pathogenicity and transmissibility of bovine H5N1 influenza virus. *Nature* <https://doi.org/10.1038/s41586-024-07766-6> (2024).
19. Good, M. R., Wei, J., Fernández-Quintero M. L., Ward A. B. & Guthmiller J. J. A single mutation in dairy cow-associated H5N1 viruses increases receptor binding breadth. Preprint at *bioRxiv* <https://doi.org/10.1101/2024.06.22.600211> (2024).
20. Nelli, R. K. et al. Sialic acid receptor specificity in mammary gland of dairy cattle infected with highly pathogenic avian influenza A(H5N1) virus. *Emerg. Infect. Dis.* **30**, 1361–1373 (2024).
21. Cox, N. J., Trock, S. C. & Burke, S. A. Pandemic preparedness and the Influenza Risk Assessment Tool (IRAT). *Curr. Top. Microbiol. Immunol.* **385**, 119–136 (2014).
22. Tool for Influenza Pandemic Risk Assessment (TIPRA) (World Health Organization, 2020).
23. Cáceres, C. J. et al. Influenza A(H5N1) virus resilience in milk after thermal inactivation. *Emerg. Infect. Dis.* **30**, 2426–2429 (2024).
24. Le Sage, V., Campbell, A. J., Reed, D. S., Duprex, W. P. & Lakdawala, S. S. Influenza H5N1 and H1N1 viruses remain infectious in unpasteurized milk on milking machinery surfaces. *Emerg. Infect. Dis.* **30**, 1335–1343 (2024).
25. Pulit-Penalosa, J. A. et al. Pathogenesis and transmission of human seasonal and swine-origin A(H1) influenza viruses in the ferret model. *Emerg. Microbes Infect.* **11**, 1452–1459 (2022).
26. Pulit-Penalosa, J. A., Belser, J. A., Tumpey, T. M. & Maines, T. R. Sowing the seeds of a pandemic? Mammalian pathogenicity and transmissibility of H1 variant influenza viruses from the swine reservoir. *Trop. Med. Infect. Dis.* **4**, 41 (2019).
27. Burrough, E. R. et al. Highly pathogenic avian influenza A(H5N1) clade 2.3.4.4b virus infection in domestic dairy cattle and cats, United States, 2024. *Emerg. Infect. Dis.* **30**, 1335–1343 (2024).
28. Arafa, A. S. et al. Risk assessment of recent Egyptian H5N1 influenza viruses. *Sci. Rep.* **6**, 38388 (2016).
29. Maines, T. R. et al. Lack of transmission of H5N1 avian-human reassortant influenza viruses in a ferret model. *Proc. Natl Acad. Sci. USA* **103**, 12121–12126 (2006).
30. Pulit-Penalosa, J. A. et al. Comparative in vitro and in vivo analysis of H1N1 and H1N2 variant influenza viruses isolated from humans between 2011 and 2016. *J. Virol.* **92**, e01444-18 (2018).
31. Roberts, K. L., Shelton, H., Stilwell, P. & Barclay, W. S. Transmission of a 2009 H1N1 pandemic influenza virus occurs before fever is detected, in the ferret model. *PLoS ONE* **7**, e43303 (2012).
32. Koster, F. et al. Exhaled aerosol transmission of pandemic and seasonal H1N1 influenza viruses in the ferret. *PLoS ONE* **7**, e33118 (2012).
33. Pulit-Penalosa, J. A. et al. Kinetics and magnitude of viral RNA shedding as indicators for influenza A virus transmissibility in ferrets. *Commun. Biol.* **6**, 90 (2023).
34. Le Sage, V. et al. Pre-existing heterosubtypic immunity provides a barrier to airborne transmission of influenza viruses. *PLoS Pathog.* **17**, e1009273 (2021).
35. Harrington, W. N., Kackos, C. M. & Webby, R. J. The evolution and future of influenza pandemic preparedness. *Exp. Mol. Med.* **53**, 737–749 (2021).
36. Long, J. S., Mistry, B., Haslam, S. M. & Barclay, W. S. Host and viral determinants of influenza A virus species specificity. *Nat. Rev. Microbiol.* **17**, 67–81 (2019).
37. Le Sage, V. et al. Pre-existing H1N1 immunity reduces severe disease with bovine H5N1 influenza virus. Preprint at *bioRxiv* <https://doi.org/10.1101/2024.10.23.619881> (2024).
38. Wang, C. et al. Sex disparities in influenza: a multiscale network analysis. *iScience* **25**, 104192 (2022).
39. Rioux, M. et al. The intersection of age and influenza severity: utility of ferrets for dissecting the age-dependent immune responses and relevance to age-specific vaccine development. *Viruses* **13**, 678 (2021).
40. Meliopoulos, V. et al. Diet-induced obesity affects influenza disease severity and transmission dynamics in ferrets. *Sci. Adv.* **10**, eadk9137 (2024).
41. Suttie, A. et al. Inventory of molecular markers affecting biological characteristics of avian influenza A viruses. *Virus Genes* **55**, 739–768 (2019).

Publisher's note Springer Nature remains neutral with regard to jurisdictional claims in published maps and institutional affiliations.

© This is a U.S. Government work and not under copyright protection in the US; foreign copyright protection may apply 2024

Methods

Viruses

The stocks of TX/37 A(H5N1), A/Nebraska/14/2019 A(H1N1) (NE/14), A/Minnesota/45/2016 A(H1N2)v (MN/45) and A/Ohio/02/2007 A(H1N1)v (OH/02) were propagated in MDCK cells at 37 °C for 48 h. The stocks of Chile/25945 A(H5N1) and A/Ohio/09/2015 A(H1N1)v (OH/09) were propagated in the allantoic cavity of 10-day-old embryonated hens' eggs at 37 °C for 24–26 h (allantoic fluid was pooled from multiple eggs). The supernatants were clarified by centrifugation, aliquoted and frozen at –80 °C. Stock titres were determined using the standard plaque assay and the stocks were sequenced and tested for exclusivity to rule out the presence of other subtypes of influenza virus. All research with highly pathogenic avian influenza viruses was conducted under biosafety level 3 containment, including enhancements required by the US Department of Agriculture and the Select Agent Program outlined in ref. 42.

Cloning and expression of recombinant HA

Genes encoding the ectodomains of the H5 HAs (residues 1 to 503 in mature protein numbering) were synthesized as codon-optimized genes (GenScript) for baculovirus expression in insect cells. HA genes were subcloned into a baculovirus transfer vector pAcGP67B (BD Biosciences), in frame with an additional carboxy-terminal thrombin site, a foldon trimerization sequence from bacteriophage T4 fibrin and a His tag⁴³. Proteins were expressed and secreted from baculovirus-infected cells, recovered from culture supernatant, and purified sequentially by metal-affinity and size-exclusion chromatography.

Glycan binding analyses

Glycan microarray printing and recombinant HA analyses have been described previously^{44,45}. Briefly, HA–antibody precomplexes were prepared by mixing recombinant HA (10 µg) with mouse anti-penta-His–Alexa Fluor 488 (Qiagen) and anti-mouse IgG–Alexa Fluor 488 (Life Technologies) antibodies in a molar ratio of 4:2:1, respectively. Complexes were allowed to form by incubating mixtures for 60 min on ice and the samples were then diluted with 500 µl PBS containing 2% (wt/vol) bovine serum albumin and streptavidin–Alexa Fluor 488 (1:1,000 (vol/vol); Life Technologies). Mixtures were applied to the microarray slides and incubated on ice for an additional 90 min. The slides were then washed by successive rinses in PBS with 0.05% Tween 20 (vol/vol), PBS and deionized water, and were then dried under a stream of nitrogen gas. Slides were scanned for fluorescence using an Innoscan 100 microarray scanner (Innopsys), and spot intensities were quantified and analysed using Mapix data acquisition and microarray image analysis software (Innopsys). Supplementary Table 1 lists the specific glycans present on the array, as well as a tabulated qualitative assessment of binding for each recombinant HA protein analysed. A second array containing only a limited set of glycans was also used for analysing glycan binding to these proteins. These glycans, a mix of linear and biantennary α2-3- and α2-6-linked sialosides of different lengths (from 1 to 4 LacNAc repeats), were imprinted on the array at different concentrations (100 µM, 20 µM, 4 µM, 0.8 µM and 0.16 µM) to assess both the specificity and avidity of α2-3- and α2-6-linked sialoside-binding proteins. This alternative glycan array slide was processed using the same procedure as described above. Supplementary Table 2 lists the glycans on the version 2 array.

Ferret experiments

Animal research was conducted under the guidance of the Centers for Disease Control and Prevention's Institutional Animal Care and Use Committee in an Association for Assessment and Accreditation of Laboratory Animal Care International-accredited animal facility. Male fitch ferrets (Triple F Farms) 7–12 months of age were used for this study. Individual animals were randomly allocated into experimental groups. No blinding was performed in any experiment.

The sample sizes were consistent with those of our previously established protocols and published work. Each animal was serologically negative for influenza A and B viruses circulating at present as confirmed by a standard haemagglutination inhibition assay. The animals were housed in stainless steel cages (56 cm (length) × 42 cm (width) × 42 cm (height)) lined with soft pellet bedding inside Duo-Flo Bioclean mobile units (Lab Products Incorporated; 150–180 air changes h⁻¹) during experimentation. Twelve ferrets were inoculated intranasally (1 ml) with 6 log₁₀[PFUs] of TX/37 H5N1 virus diluted in PBS. Transmissibility of the virus was assessed by pairing naïve ferrets with inoculated ferrets (ratio 1:1) 24 h p.i. In the direct contact transmission model, a naïve ferret was placed in the same cage as an inoculated ferret (three ferret pairs). In the respiratory droplet transmission model, a naïve ferret was placed in an adjacent cage with perforated walls between cages facilitating air exchange but eliminating contact between the donor and naïve ferrets (six ferret pairs)²⁹. In the fomite transmission model, a naïve ferret and inoculated ferret swapped cages once daily (until euthanasia of the donors; two cage swaps) so that the contact animal was exposed to stainless steel cage walls, bedding, food and water that had been in direct contact with an inoculated ferret shedding virus into that environment through respiratory secretions, faeces and virus-laden aerosols. Before the swap, the cage housing an inoculated ferret was swabbed using two cotton swabs pre-moistened with PBS (one continuous movement across all four stainless steel cage walls, cage floor and stainless steel water bottle tube)⁷. To detect virus in aerosolized fomites, air samples were collected from cages for 1 h at 3.5 l min⁻¹ (210 l total air collection volume) using the National Institute for Occupational Safety and Health BC 251 two-stage cyclone aerosol sampler^{46,47} (the experimental design is shown in Extended Data Fig. 7a). The cage swab and air samples were split and frozen at –80 °C until titration in MDCK cells or used for RNA extraction to evaluate viral RNA copy titres in each sample. In each transmission experiment, all naïve contact animals were housed in a separate Duo-Flo Bioclean unit before establishing contact with the inoculated animals, which took place 24 h after inoculation. Following inoculation or contact, all of the ferrets were observed daily for clinical signs of infection. Lethargy was measured on the basis of a scoring system of 0 to 3, which was used to calculate a relative inactivity index^{48,49}. Animals that exhibited sustained diarrhoea, lethargy and laboured breathing, in addition to other signs of severe disease, were humanely euthanized. NWs and RSs were collected from all inoculated and contact ferrets every 1–2 days, and conjunctival washes were collected from six representative virus-inoculated ferrets on day 1 and 3 p.i. (ref. 50). To determine the kinetics of viraemia, blood samples were collected from three representative virus-inoculated ferrets on days 1 and 2 p.i. Four inoculated ferrets were euthanized on day 3 p.i. for the assessment of virus replication and systemic spread of the virus⁵¹. Similarly, all contact animals that developed severe disease were euthanized (3–9 p.c.) and assessed for systemic spread of virus in tissues. All of the ferret samples were frozen at –80 °C and titred in MDCK cells. A separate series of experiments were performed to further validate the fomite transmission model using human seasonal and swine-origin viruses (NE/14 A(H1N1), MN/45 A(H1N2)v, OH/09 A(H1N1)v and OH/02 A(H1N1)v), which were previously shown to transmit efficiently in the direct contact model^{25,52,53}. Three ferrets per group were challenged intranasally (1 ml) with 6 log₁₀[PFUs] of the respective virus diluted in PBS. Three ferret pairs were tested per virus, cage swaps were performed daily for 5 consecutive days, and cage swabs and NWs were performed and processed as described above.

Aerosol collection

Three to five ferrets per group were inoculated intranasally (1 ml) with 6 log₁₀[PFUs] of TX/37, Chile/25945, NE/14 and MN/45 virus diluted in PBS. Alert ferrets were individually placed in disinfected, vented transport containers (solid walls with perforated lid; 23.9 l in size) and air was collected for 1 h using a National Institute for Occupational Safety

Article

and Health BC 251 two-stage cyclone aerosol sampler (at 3.5 l min^{-1})^{46,47} and a SPOT sampler, sequentially (Series 110B, Handix Scientific) (at 1.5 l min^{-1}). The samples were collected at the same time of the day. BC 251 samplers fractionated air particles into three fractions on the basis of particle diameter: >4 µm, 1–4 µm and <1 µm. The SPOT sampler collected airborne particles into one sample. Following collection, part of each sample was inactivated in AVL buffer (Qiagen) according to the manufacturer's protocol to quantify viral RNA copies (most RNA was recovered in the >4-µm fraction of the BC 251 sampler, as reported previously³³, and the presented data represent the sum from the three fractions). The remaining sample was immediately evaluated for infectious virus titre by plaque assay (no infectious virus was recovered from the fractions containing particles of 1–4 µm or <1 µm; therefore, the data represent infectious virus recovered in the >4-µm fraction of the BC 251 sampler). To normalize between the samplers, the data are presented as viral titre per hour of collection. Samplers were decontaminated with 70% ethanol and air-dried after each sampling day. Transport containers were thoroughly decontaminated with 70% ethanol after each use.

Next-generation sequencing

Viral RNA was extracted using the QIAamp Viral RNA Mini Kit or RNeasy plus kit (Qiagen) and processed for influenza genome amplification and next-generation sequencing as previously described⁴⁶ with the slight modification of using 100× coverage and a 50-bp N spacer between TX/37 reference gene segments using Geneious Prime V2020.2.4. Next-generation sequencing data have been deposited in the Sequence Read Archive of the National Center for Biotechnology Information, under the BioProject accession number PRJNA1128668.

Statistical analysis

Analyses were conducted in R version 4.4.0. Data were tested for normality using Shapiro–Wilk test (`shapiro.test` in R). Upon finding inconsistent validation of normality, a non-parametric Kruskal–Wallis test (`kruskal.test` in R) was performed. Results between BC 251 and SPOT samplers were not statistically different, and data were combined for further analysis. A Kruskal–Wallis test was used to examine the difference between viruses for each day of sample collection (days 1 and 2; NW and air sample titres). Kruskal–Wallis tests that showed statistical significance ($P < 0.05$) were followed up with a Dunn's post hoc test with Bonferroni's correction for multiple pairwise comparisons using the `dunnTest` function in the FSA v0.9.5 R package⁵⁴.

Reporting summary

Further information on research design is available in the Nature Portfolio Reporting Summary linked to this article.

Data availability

Next-generation sequencing data have been deposited in the Sequence Read Archive of the National Center for Biotechnology Information

under the BioProject accession number PRJNA1128668. Genome sequences of TX/37 are publicly available from GenBank (under the accession numbers PP577940–PP577947) and GISAID (under the accession number EPI_ISL_19027114). Source data are provided with this paper.

42. Meechan, P. J. & Potts, J. *Biosafety in Microbiological and Biomedical Laboratories* 6th edn (Centers for Disease Control and Prevention & National Institutes of Health, 2020); <https://stacks.cdc.gov/view/cdc/97733>.
43. Stevens, J. et al. Structure of the uncleaved human H1 hemagglutinin from the extinct 1918 influenza virus. *Science* **303**, 1866–1870 (2004).
44. Yang, H. et al. Molecular characterizations of surface proteins hemagglutinin and neuraminidase from recent H5Nx avian influenza viruses. *J. Virol.* **90**, 5770–5784 (2016).
45. Yang, H., Carney, P. J., Chang, J. C., Villanueva, J. M. & Stevens, J. Structural analysis of the hemagglutinin from the recent 2013 H7N9 influenza virus. *J. Virol.* **87**, 12433–12446 (2013).
46. Pulit-Penalosa, J. A. et al. Comparative assessment of severe acute respiratory syndrome coronavirus 2 variants in the ferret model. *mBio* **13**, e0242122 (2022).
47. Blachere, F. M. et al. Measurement of airborne influenza virus in a hospital emergency department. *Clin. Infect. Dis.* **48**, 438–440 (2009).
48. Reuman, P. D., Keely, S. & Schiff, G. M. Assessment of signs of influenza illness in the ferret model. *J. Virol. Methods* **24**, 27–34 (1989).
49. Zitzow, L. A. et al. Pathogenesis of avian influenza A (H5N1) viruses in ferrets. *J. Virol.* **76**, 4420–4429 (2002).
50. Belser, J. A. et al. Influenza virus respiratory infection and transmission following ocular inoculation in ferrets. *PLoS Pathog.* **8**, e1002569 (2012).
51. Maines, T. R. et al. Avian influenza (H5N1) viruses isolated from humans in Asia in 2004 exhibit increased virulence in mammals. *J. Virol.* **79**, 11788–11800 (2005).
52. Belser, J. A. et al. Pathogenesis and transmission of triple-reassortant swine H1N1 influenza viruses isolated before the 2009 H1N1 pandemic. *J. Virol.* **85**, 1563–1572 (2011).
53. Pulit-Penalosa, J. A. et al. Antigenically diverse swine origin H1N1 variant influenza viruses exhibit differential ferret pathogenesis and transmission phenotypes. *J. Virol.* <https://doi.org/10.1128/JVI.00095-18> (2018).
54. Ogle, D. H., Doll, J. C., Powell Wheeler, A. & Dinno, A. FSA: Simple fisheries stock assessment methods. R package version 4.4.0 <https://CRAN.R-project.org/package=FSA> (2023).

Acknowledgements We thank the Comparative Medicine Branch at the Centers for Disease Control and Prevention for care of the animals used in this study; Public Health Region 1 of the Texas Department of State Health Services, the Texas Tech University Bioterrorism Response Laboratory in Lubbock, TX and the Texas Department of State Health Services for access to the human sample from which TX/37 was isolated; and the research institutes that have provided sequence data used in this study and for making this information publicly available in GISAID and GenBank. Glycan microarrays were produced under contract by J. Paulson. The findings and conclusions in this report are those of the authors and do not necessarily represent the official position of the Centers for Disease Control and Prevention and the Agency for Toxic Substances and Disease Registry.

Author contributions J.A.P.-P. designed and optimized aerosol collection procedures, performed ferret experiments, processed samples and analysed data. J.A.B., N.B., C.P., X.S. and T.R.M. performed ferret experiments and processed ferret samples. T.J.K. and X.S. performed sequence analysis. T.J.K. performed statistical analysis. H.Z. assisted with plaque assays. P.C., J.C. and B.B.-F. produced the recombinant HA and performed receptor binding experiments. J.S. performed receptor binding data analysis. J.A.D.L.C. and Y.H. isolated and characterized the virus under the supervision of H.D. and C.T.D., J.A.P.-P. and J.A.B. wrote the initial draft of the manuscript with input from T.R.M., T.M.T. and J.S. who also supervised the work. All authors reviewed and approved the manuscript.

Competing interests The authors declare no competing interests.

Additional information

Supplementary information The online version contains supplementary material available at <https://doi.org/10.1038/s41586-024-08246-7>.

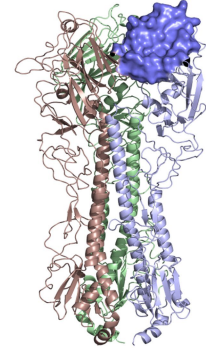
Correspondence and requests for materials should be addressed to Joanna A. Pulit-Penalosa.

Peer review information *Nature* thanks the anonymous reviewers for their contribution to the peer review of this work.

Reprints and permissions information is available at <http://www.nature.com/reprints>.

A

H3 Numbering	98	131	139	145/6	153	159	183	195	219	229
H5 Numbering	91	126	134	141/2	149	155	179	192	215	225
A/Texas/37/2024_H5N1#	-Y-	-ETSLGVSA-	-PS-	-WLIKKN-	-HHSNNAAEQTNL-	-YK-	-TRSQVNGQR-	-	-	-
A/Michigan/90/2024_H5N1#	-.-	-	-	-	-	-	-	-	-	-
A/Colorado/109/2024_H5N1#	-.-	-	-	-	-	-	-	-	-	-
A/Dairy Cow/NM/A240920343-93/24_H5N1#	-.-	-	-	-	-	-	-	-	-	-
Dairy Cow consensus H5N1#	-.-	-	-	-	-	-	-	-	-	-
A/Chile/25945/2023_H5N1	-.-	-	-	-	-	-	-	-	-	-
A/Astrakhan/3212/2020_H5N8*	-.-	-	-	-	-	-	-	-	-	-
A/Sichuan/06681/2021_H5N6*	-.-	-	-	-	-V-	-	-I-	-	-	-
A/gyrfalcon/WA/41088-6/2014_H5N8†	-.-	-	-	-S-	-	-A-	-	-S-	-	-
A/Nthn pintail/WA/40964/2014_H5N2†	-.-	-	-	-S-	-	-A-	-	-S-	-	-
A/Sichuan/26221/2014_H5N6†	-.-	-	-	-	-	-A-	-	-	-	-
A/Vietnam/1203/2004_H5N1*	-.-	-A...S-	-S-	-ST-	-P.D.A..K.Q-	-	-K...S..-	-	-	-
A/Switzerland/9715293/2013_H3N2*	-.-	-TQN...T.SS-	-S-	-THL.S-	-PGTDKD.IF..A-	-	-SPRIDIIPS.-	-	-	-

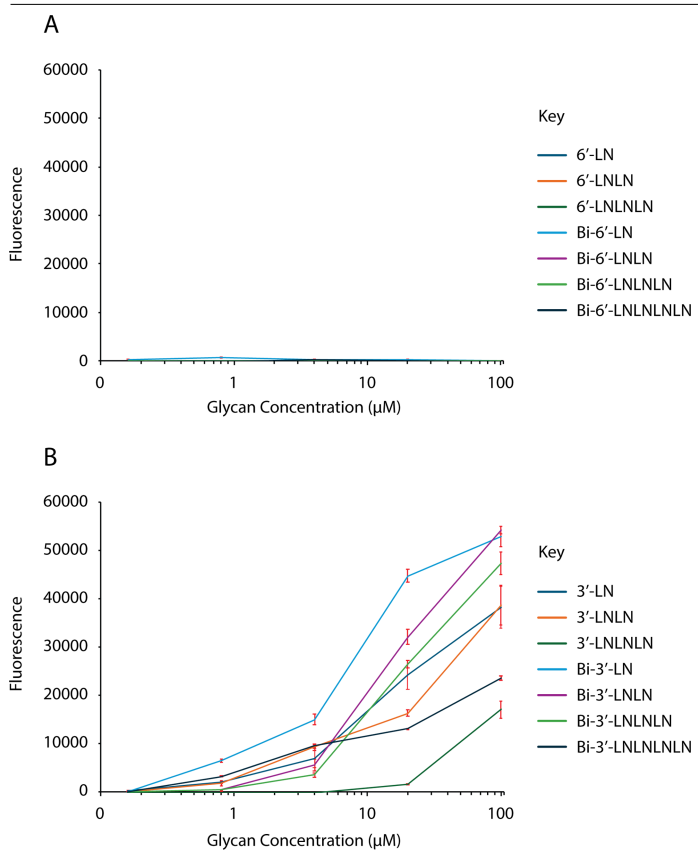
**B**

H5 Numbering	1	50
A/Texas/37/2024_H5N1#	-	DQICIGYHAN NSTEQVDTIM EKNVTVTHAQ DILEKTHNGK LCDLNGVKPL
A/Michigan/90/2024_H5N1#	-	-
A/Colorado/109/2024_H5N1#	-	-
A/Dairy Cow/NM/A240920343-93/24_H5N1#	-	-
H5 Numbering	31	110
A/Texas/37/2024_H5N1#	ILKDCSVAGW	LLGNPMCDEF IRVPEWSYIV ERANPANDLC YPGSLNDYEE LKHMLSRINH
A/Michigan/90/2024_H5N1#	-	-
A/Colorado/109/2024_H5N1#	-	-
A/Dairy Cow/NM/A240920343-93/24_H5N1#	-	-
H5 Numbering	111	170
A/Texas/37/2024_H5N1#	FEKIQIIPKS	SWPNHETSLG VSAACPYQGA PSFFRNVVWL IKKNDAYPTI KISYNNTNRE
A/Michigan/90/2024_H5N1#	-	-
A/Colorado/109/2024_H5N1#	-	-
A/Dairy Cow/NM/A240920343-93/24_H5N1#	-	-
H5 Numbering	171	230
A/Texas/37/2024_H5N1#	DLILWGIHH	SNNAEEQTNL YKNPITYISV GTSTLNQRLA PKIATRSQVN GQRGRMDFFW
A/Michigan/90/2024_H5N1#	-	-
A/Colorado/109/2024_H5N1#	-	-
A/Dairy Cow/NM/A240920343-93/24_H5N1#	-	-
H5 Numbering	231	290
A/Texas/37/2024_H5N1#	TILKPDDAIH	FESNGNFIAP EYAYKIVKKG DSTIMKSGVE YGHCNTKCQT PVGAINSSMP
A/Michigan/90/2024_H5N1#	-	-
A/Colorado/109/2024_H5N1#	-	-
A/Dairy Cow/NM/A240920343-93/24_H5N1#	-	-
H5 Numbering	291	329
A/Texas/37/2024_H5N1#	FHNIIHPLTIG	ECPKYVKSNSK LVLATGLRNS PLREKRRK-R
A/Michigan/90/2024_H5N1#	-	-
A/Colorado/109/2024_H5N1#	-	-
A/Dairy Cow/NM/A240920343-93/24_H5N1#	-	-

Extended Data Fig. 1 | Comparison of receptor binding site residues in diverse H5 HAs. (A) Sequence residues that comprise the TX/37 HA receptor binding site (RBS) aligned with HA sequences from this and a previous study⁴⁴, as well as with a recent bovine A(H5N1) virus sequence that reported both human and avian receptor binding¹⁸. Alignments with amino acid positions (H3 and H5 numbering) are indicated above the alignment. Conserved residues are indicated as dots. The position of the RBS on the HA is illustrated on the TX/37

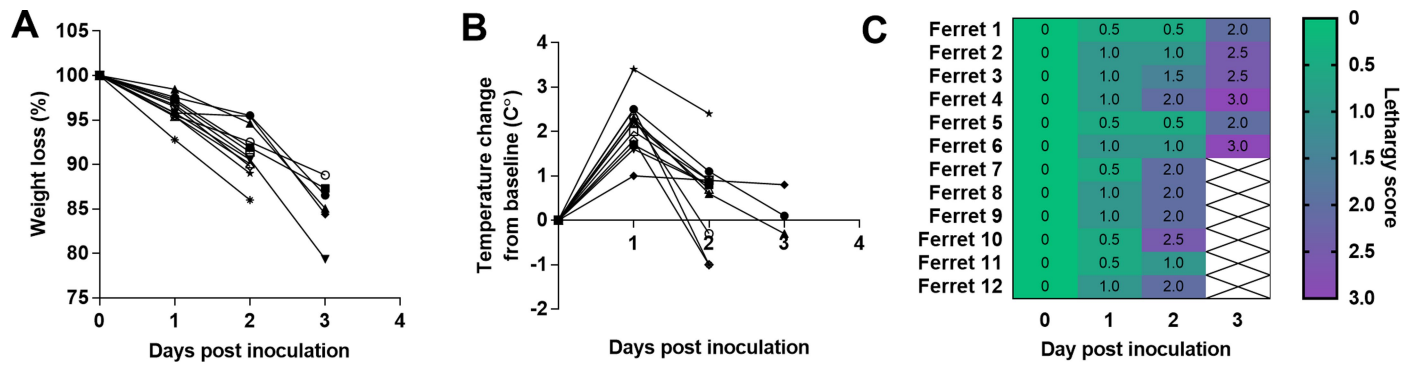
structural model. The HA is illustrated as a cartoon, while the receptor binding site residues listed in the alignment are shown as a surface representation. Figure was generated using PyMol 2.5.5. *Current data. †HAs with published glycan array binding results. #Isolates associated with dairy farm outbreaks including dairy cow isolate consensus sequence. (B) Full alignment of the HA for all viruses associated with dairy farm outbreaks included in A.

Article



Extended Data Fig. 2 | Glycan microarray analysis of the TX/37 recHA.

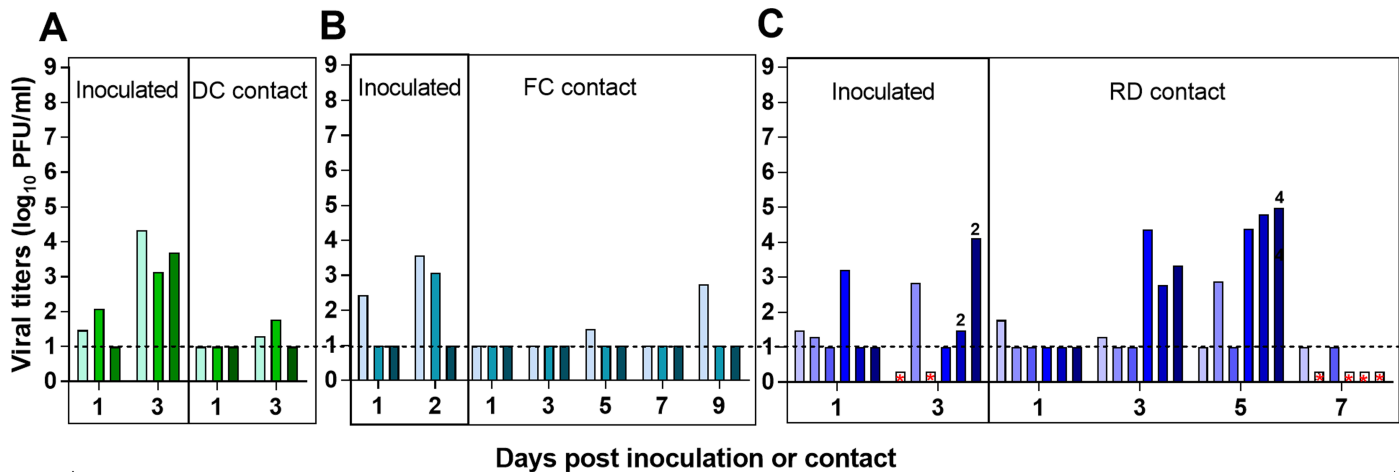
A second glycan array containing only a limited set of linear and biantennary (A) α 2-6 and (B) α 2-3 linked sialosides of different lengths (from 1 to 4 LacNAc repeats), printed onto the array at different concentrations, were used to assess both HA binding specificity and avidity of the TX/37 recHA. Error bars are standard deviations from six independent replicates on the array. Each of the glycans' structures are listed in Supplemental Table 2.



Extended Data Fig. 3 | Changes in body weight, temperature, and lethargy in ferrets inoculated intranasally with $6 \log_{10} [\text{PFUs}]$ of TX/37. (A) Percent weight loss from pre-inoculation baseline body weight. (B) Body temperature

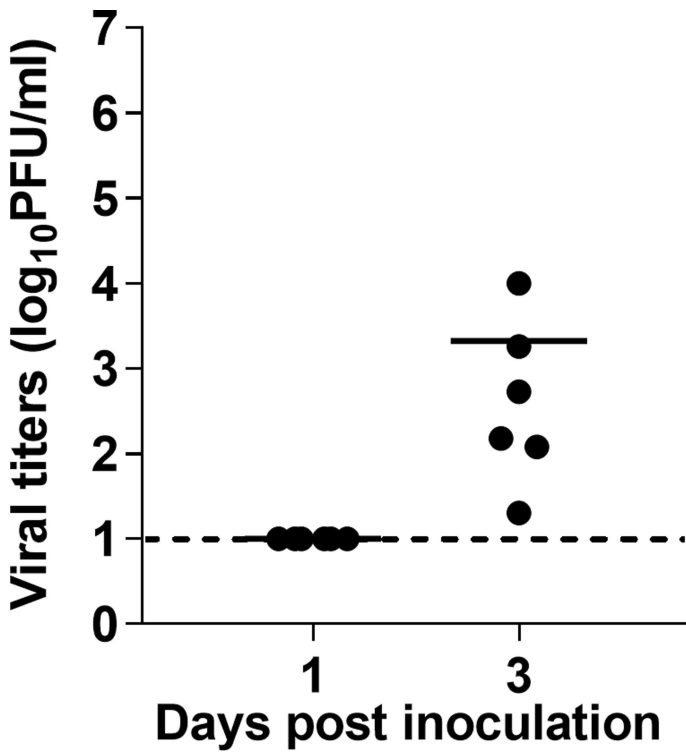
change from pre-inoculation baseline temperature. Time courses for individual ferrets are shown up to the day of euthanasia (days 2-3), $n = 12$. (C) Lethargy was evaluated based on a scoring system of 0 to 3.

Article



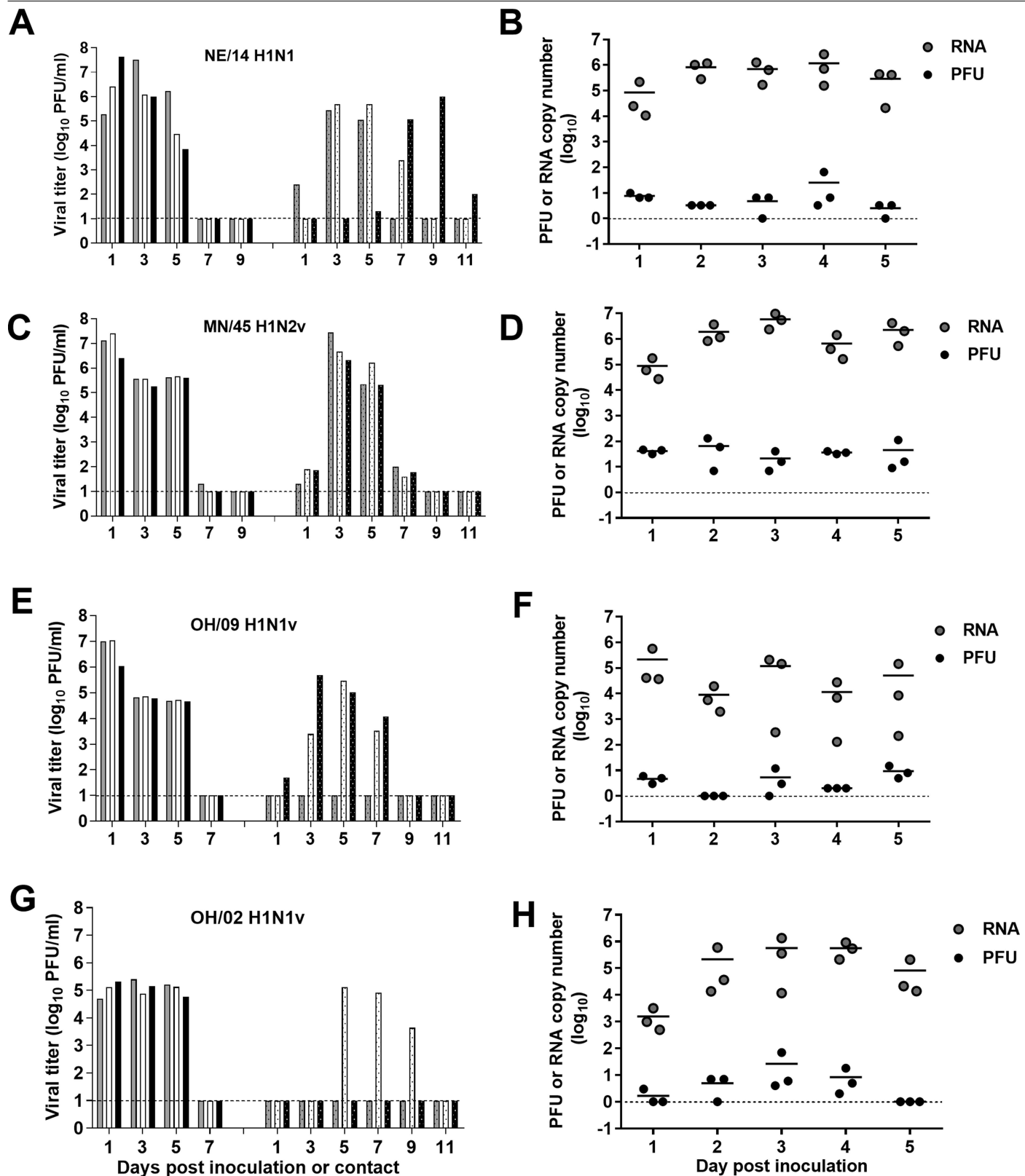
Extended Data Fig. 4 | Viral titers in rectal swabs collected from inoculated and contact ferrets. Twelve ferrets were inoculated intranasally with $6 \log_{10}$ [PFUs] of TX/37 virus. Transmission to naive contacts in (A) direct contact transmission (DC), (B) fomite transmission (FC), and (C) respiratory droplet transmission (RD) settings were established, and rectal swabs were collected every other day post-inoculation or contact, or on the day of euthanasia (day

or day 4 indicated on top of the bar). Rectal swab titers for the inoculated animals are shown on the left side of each graph, and rectal swab titers for contact animals are shown on the right side of each graph. Red asterisks denote animals that succumbed to infection prior to sample collection. The limit of detection is 10 PFU/ml, dashed line. Each bar represents an individual ferret.



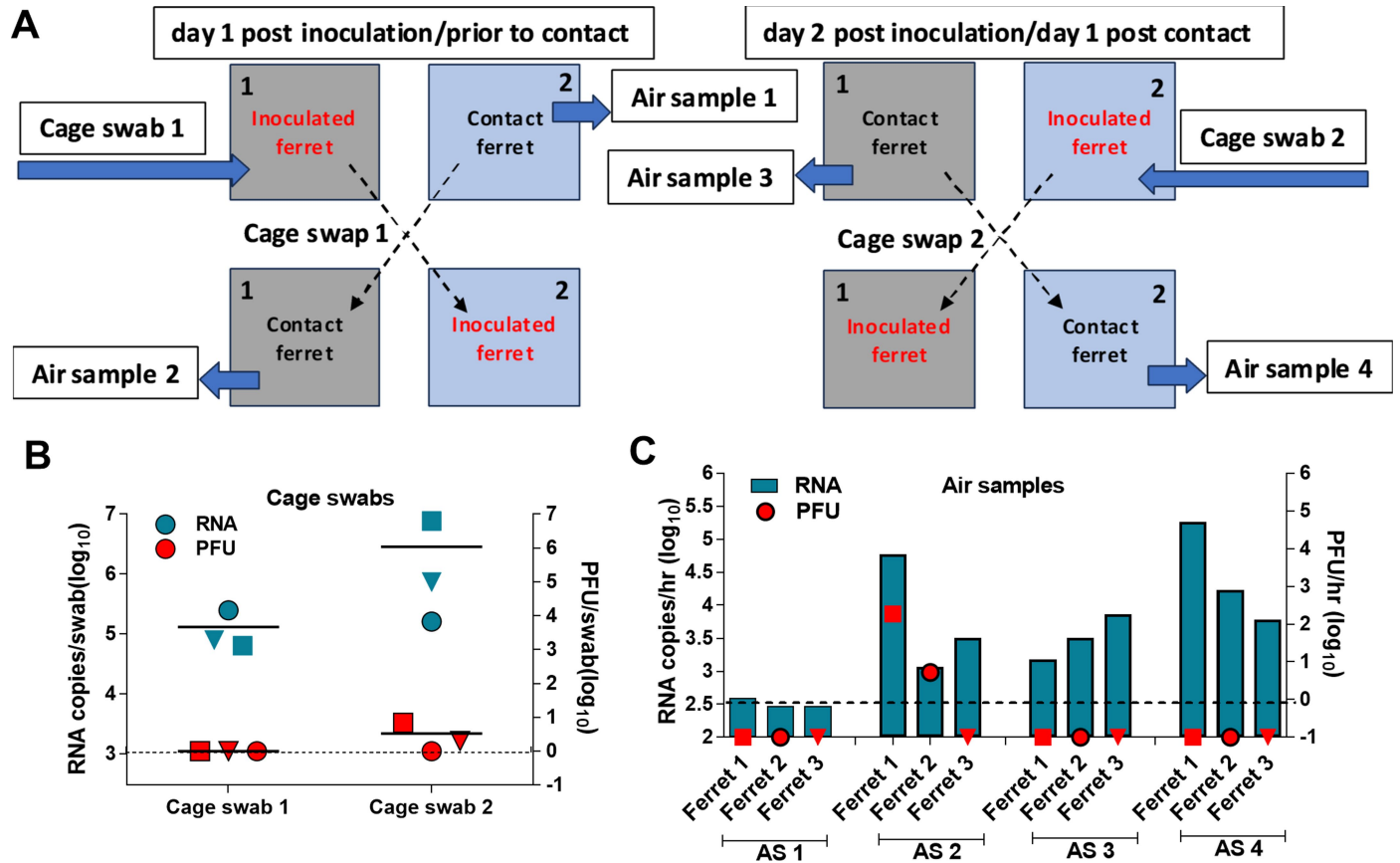
Extended Data Fig. 5 | Viral titers in conjunctival wash samples from ferrets inoculated with 6 log₁₀ [PFUs] of TX/37 A(H5N1) virus. Conjunctival washes collected from inoculated ferrets (n = 6). The samples were titrated in MDCK cells. The limit of detection is 10 PFU/ml, dashed line. Each symbol represents an individual ferret.

Article



Extended Data Fig. 6 | Transmission of H1 subtype viruses in the ferret fomite model. Three ferrets per group were inoculated with $6 \log_{10}$ [PFUs] of (A, B) human seasonal NE/14 A(H1N1), (C, D) swine-origin MN/45 A(H1N2)v, (E, F) swine-origin OH/09 A(H1N1)v, (G, H) or swine-origin OH/02 A(H1N1) viruses. The transmission experiment was conducted for 5 days (5 cage swaps). (A, C, E, G) Titers in nasal washes collected from inoculated animals (left graph

side), and contact (right graph side) are expressed as \log_{10} [PFU/ml]. The limit of detection is 10 PFU (dashed line). (B, D, F, H) Each cage was swabbed prior to cage swap. Infectious virus titers and RNA copy number titers in cage swabs are expressed as \log_{10} [PFU or RNA/swab]. Limit of detection is 1 PFU (dashed line), and $2.9 \log_{10}$ [RNA copies]. Each bar and symbol represent an individual ferret.

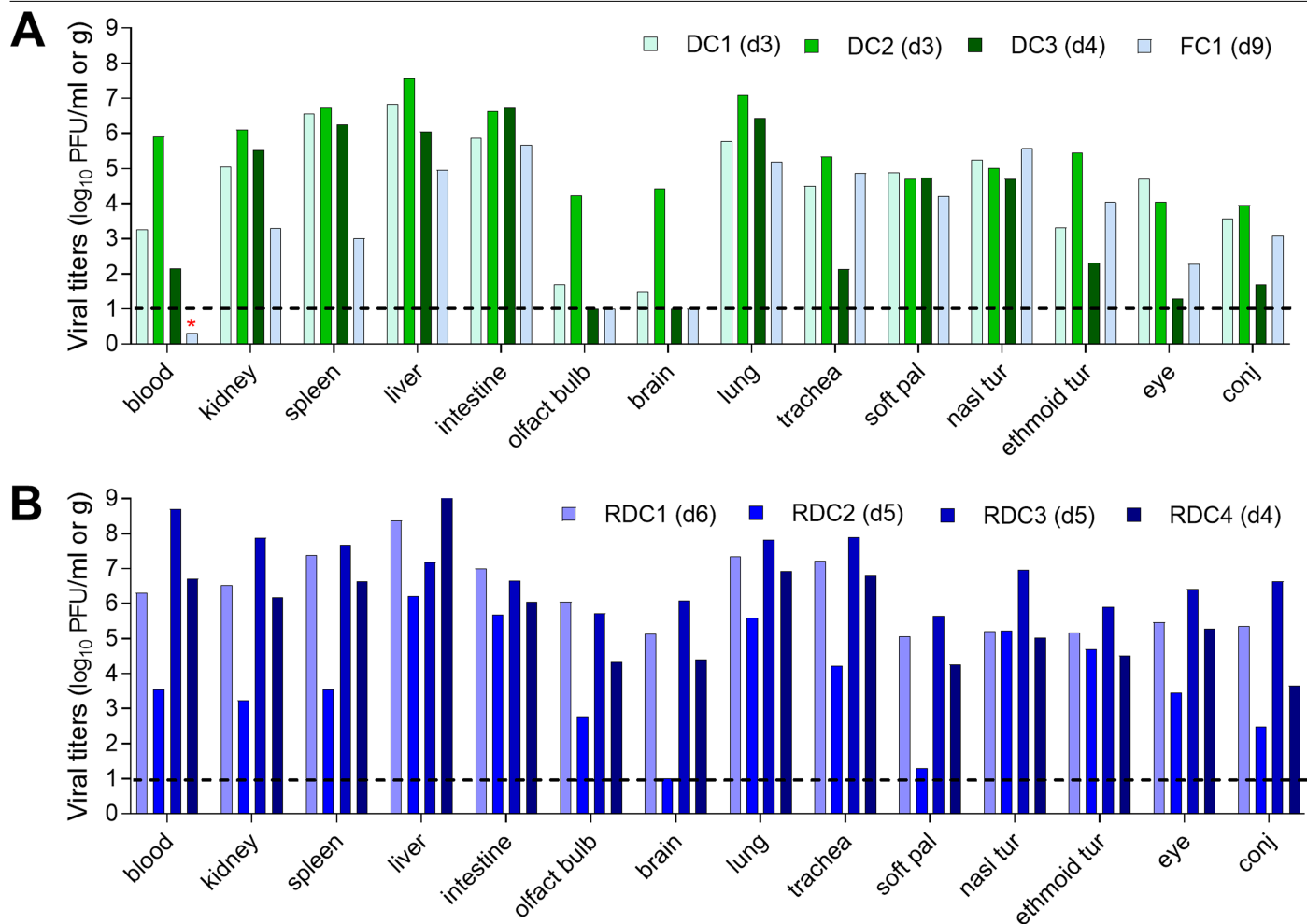


Extended Data Fig. 7 | Detection of infectious TX/37 A(H5N1) on fomites.

(A) Experimental design ($n = 3$). A ferret inoculated with $6 \log_{10}$ of TX/37 A(H5N1) was placed in cage 1 (grey), and a naive ferret was placed in cage 2 (blue). Twenty-four hours post inoculation a cage swab was collected from the cage housing each of the inoculated ferrets (cage 1). An air sample was collected (1 h using BC 251 samplers) from each cage housing the naive ferret [cage 2, air sample 1 (AS1)]. Following cage swap, air sample was collected from cage 1 which now housed the respective contact ferret [air sample 2 (AS2)]. The process was repeated the next day [cage swap 2, air sample 3 (AS3), and air sample 4 (AS4)]. (B) Infectious virus titers and RNA copy number titers in cage

swabs are expressed as \log_{10} [PFU or RNA copies/swab]. Limit of detection is 1 PFU, and $2.9 \log_{10}$ [RNA copies]. (C) Infectious virus titers in air samples are expressed as \log_{10} [PFU/hour] (red symbols; limit of detection 1 PFU/hour; the data represents infectious virus recovered in the $>4 \mu\text{m}$ fraction of the BC 251 sampler, no infectious virus was recovered from the fractions containing particles of $1-4 \mu\text{m}$, or $<1 \mu\text{m}$). Viral RNA copy titers in air samples are expressed as \log_{10} RNA copies/hour (bars; limit of detection $2.5 \log_{10}$ RNA copies/hour; data represents the sum from the three sampler fractions). Each ferret is represented by a different symbol and the order of ferrets corresponds to the order of ferrets in Figure 2b.

Article



Extended Data Fig. 8 | Tissue distribution of TX/37 H5N1 in infected contact ferrets. Virus dissemination to tissues collected from contacts in the (A) direct contact (DC) and fomite (FC), and (B) respiratory droplet transmission (RDC) set-ups. Viral titers were obtained using standard plaque assay and are reported at \log_{10} [PFU/ml] [blood, soft palate (soft pal), nasal turbinates (nasal tur), ethmoid turbinates (ethmoid tur), eye, conjunctiva (conj)] or \log_{10} [PFU/g]

of tissue] [kidney, spleen, liver, intestines, olfactory bulb (olfact bulb), brain, lungs, trachea]. The red asterisk indicate a sample that was not collected. Days post contact on which the samples were collected are shown in parentheses. The limit of detection is 10 PFU/ml or g, dashed line. Colors correspond to the contact ferrets in Figure 2a–c. Each bar represents an individual ferret.

Corresponding author(s): Pulit-Penalosa, Joanna

Last updated by author(s): 09/28/2024

Reporting Summary

Nature Portfolio wishes to improve the reproducibility of the work that we publish. This form provides structure for consistency and transparency in reporting. For further information on Nature Portfolio policies, see our [Editorial Policies](#) and the [Editorial Policy Checklist](#).

Statistics

For all statistical analyses, confirm that the following items are present in the figure legend, table legend, main text, or Methods section.

n/a Confirmed

- The exact sample size (n) for each experimental group/condition, given as a discrete number and unit of measurement
- A statement on whether measurements were taken from distinct samples or whether the same sample was measured repeatedly
- The statistical test(s) used AND whether they are one- or two-sided
Only common tests should be described solely by name; describe more complex techniques in the Methods section.
- A description of all covariates tested
- A description of any assumptions or corrections, such as tests of normality and adjustment for multiple comparisons
- A full description of the statistical parameters including central tendency (e.g. means) or other basic estimates (e.g. regression coefficient) AND variation (e.g. standard deviation) or associated estimates of uncertainty (e.g. confidence intervals)
- For null hypothesis testing, the test statistic (e.g. F , t , r) with confidence intervals, effect sizes, degrees of freedom and P value noted
Give P values as exact values whenever suitable.
- For Bayesian analysis, information on the choice of priors and Markov chain Monte Carlo settings
- For hierarchical and complex designs, identification of the appropriate level for tests and full reporting of outcomes
- Estimates of effect sizes (e.g. Cohen's d , Pearson's r), indicating how they were calculated

Our web collection on [statistics for biologists](#) contains articles on many of the points above.

Software and code

Policy information about [availability of computer code](#)

Data collection N/A

Data analysis N/A

For manuscripts utilizing custom algorithms or software that are central to the research but not yet described in published literature, software must be made available to editors and reviewers. We strongly encourage code deposition in a community repository (e.g. GitHub). See the Nature Portfolio [guidelines for submitting code & software](#) for further information.

Data

Policy information about [availability of data](#)

All manuscripts must include a [data availability statement](#). This statement should provide the following information, where applicable:

- Accession codes, unique identifiers, or web links for publicly available datasets
- A description of any restrictions on data availability
- For clinical datasets or third party data, please ensure that the statement adheres to our [policy](#)

NGS sequence data have been deposited to NCBI Sequence Read Archive under BioProject ID: PRJNA1128668

Research involving human participants, their data, or biological material

Policy information about studies with [human participants or human data](#). See also policy information about [sex, gender \(identity/presentation\), and sexual orientation](#) and [race, ethnicity and racism](#).

Reporting on sex and gender	<input type="text" value="N/A"/>
Reporting on race, ethnicity, or other socially relevant groupings	<input type="text" value="N/A"/>
Population characteristics	<input type="text" value="N/A"/>
Recruitment	<input type="text" value="N/A"/>
Ethics oversight	<input type="text" value="N/A"/>

Note that full information on the approval of the study protocol must also be provided in the manuscript.

Field-specific reporting

Please select the one below that is the best fit for your research. If you are not sure, read the appropriate sections before making your selection.

Life sciences Behavioural & social sciences Ecological, evolutionary & environmental sciences

For a reference copy of the document with all sections, see nature.com/documents/nr-reporting-summary-flat.pdf

Life sciences study design

All studies must disclose on these points even when the disclosure is negative.

Sample size	<input type="text" value="Ferret animal model used, 3-6 ferrets per group"/>
Data exclusions	<input type="text" value="N/A"/>
Replication	<input type="text" value="3-12 outbred ferrets were used per group, the experiments were not repeated to avoid unnecessary animal use in accordance to the the Rs guidelines"/>
Randomization	<input type="text" value="random animal distribution, outbred species"/>
Blinding	<input type="text" value="N/A"/>

Reporting for specific materials, systems and methods

We require information from authors about some types of materials, experimental systems and methods used in many studies. Here, indicate whether each material, system or method listed is relevant to your study. If you are not sure if a list item applies to your research, read the appropriate section before selecting a response.

Materials & experimental systems

n/a	Involved in the study
<input checked="" type="checkbox"/>	<input type="checkbox"/> Antibodies
<input checked="" type="checkbox"/>	<input type="checkbox"/> Eukaryotic cell lines
<input checked="" type="checkbox"/>	<input type="checkbox"/> Palaeontology and archaeology
<input type="checkbox"/>	<input checked="" type="checkbox"/> Animals and other organisms
<input checked="" type="checkbox"/>	<input type="checkbox"/> Clinical data
<input checked="" type="checkbox"/>	<input type="checkbox"/> Dual use research of concern
<input checked="" type="checkbox"/>	<input type="checkbox"/> Plants

Methods

n/a	Involved in the study
<input checked="" type="checkbox"/>	<input type="checkbox"/> ChIP-seq
<input checked="" type="checkbox"/>	<input type="checkbox"/> Flow cytometry
<input checked="" type="checkbox"/>	<input type="checkbox"/> MRI-based neuroimaging

Animals and other research organisms

Policy information about [studies involving animals](#); [ARRIVE guidelines](#) recommended for reporting animal research, and [Sex and Gender in Research](#)

Laboratory animals	Male ferrets ,7 month old (Triple Farms)
Wild animals	N/A
Reporting on sex	Male ferrets were used throughout the study. No sex based analysis were performed.
Field-collected samples	N/A
Ethics oversight	Animal research was conducted under the guidance of the Centers for Disease Control and Prevention's Institutional Animal Care and Use Committee in an Association for Assessment and Accreditation of Laboratory Animal Care International-accredited animal facility

Note that full information on the approval of the study protocol must also be provided in the manuscript.

Plants

Seed stocks	N/A
Novel plant genotypes	N/A
Authentication	N/A